https://doi.org/10.5194/egusphere-2024-14
Preprint. Discussion started: 29 January 2024

Unravelling Disparities in Eulerian and Lagrangian Moisture Tracking Models in Monsoon- and Westerlies-dominated Basins Around the Tibetan Plateau

Ying Li[1,2,3], Chenghao Wang[4,5], Qiuhong Tang[6], Shibo Yao[7], Bo Sun[8], Hui Peng[1], and Shangbin Xiao[1,2,3]

[1] College of Hydraulic and Environmental Engineering, China Three Gorges University, Yichang, China
[2] Engineering Research Center of Eco-environment in Three Gorges Reservoir Region, Yichang, China
[3] Three Gorges Reservoir Ecosystem Field Scientific Observation and Research Station, China Three Gorges University, Yichang, China
[4] School of Meteorology, University of Oklahoma, Norman, OK, USA
[5] Department of Geography and Environmental Sustainability, University of Oklahoma, Norman, OK, USA
[6] Key Laboratory of Water Cycle and Related Land Surface Processes, Institute of Geographic Sciences and Natural Resources Research, Chinese Academy of Sciences, Beijing, China
[7] China Meteorological Administration Key Laboratory for Climate Prediction Studies, National Climate Center, Beijing, China
[8] Collaborative Innovation Center on Forecast and Evaluation of Meteorological Disasters/Key Laboratory of Meteorological Disasters, Ministry of Education/Joint International Research Laboratory of Climate and Environment Change, Nanjing University of Information Science and Technology, Nanjing, China

Correspondence to: Ying Li (ly_hydro@outlook.com) and Shangbin Xiao (shangbinx@163.com)

Abstract. Beyond traditional meteorological and (paleo)climatological analyses, numerical moisture tracking provides a quantitative diagnosis of moisture sources to the Tibetan Plateau (TP). While existing studies predominantly employ either the Eulerian or Lagrangian method, the potential differences in their simulations and the underlying causes of these discrepancies remain unexplored. In this study, we compare the applications of the most widely used Eulerian (WAM-2layers) and Lagrangian (FLEXPART-WaterSip) models in the TP, specifically in an Indian Summer Monsoon (ISM)-dominated basin (Yarlung Zangbo River Basin, YB) and a westerlies-dominated basin (upper Tarim River Basin, UTB). Compared to FLEXPART-WaterSip, WAM-2layers generally estimates higher moisture contributions from westerlies-dominated and distant source regions but lower contributions from local recycling. However, WAM-2layers simulations can be improved by using higher spatial-temporal resolution forcing data. The inherent ability in WAM-2layers to distinguish between evaporation and precipitation makes it more effectively in identifying varying moisture contributions arising from distinct surface evaporation sources. In contrast, in regions heavily influenced by smaller-scale convective systems with high spatial heterogeneity, such as the UTB when compared to the YB, simulations from FLEXPART-WaterSip tend to be more reliable. However, FLEXPART-WaterSip is prone to introducing additional errors when using specific humidity information in particles to infer moisture uptake and loss, although it accurately depicts the three-dimensional movement of air particles.

https://doi.org/10.5194/egusphere-2024-14
Preprint. Discussion started: 29 January 2024

1 Introduction

Moisture tracking through numerical models play a pivotal role in advancing our quantitative understanding of the global and regional atmospheric water cycle, and is crucial for a variety of applications in meteorology, hydrology, and climate science (Gimeno et al., 2012; Gimeno et al., 2020). Numerical models for moisture tracking can be broadly classified into two categories: Eulerian and Lagrangian methods. The Eulerian method generally employs a fixed spatial grid system with predefined grid spacing, and primarily focuses on averaged physical quantities over the atmospheric domain. Eulerian models simulate the movement and alteration of water vapor between adjacent grid cells by solving a system of water balance equations. Leveraging the discrete nature of grid cells to simplify numerical computations, they are well suited for describing large-scale hydrological circulations (van der Ent et al., 2014; Link et al., 2020). In comparison, the Lagrangian method employs a particle trajectory tracking approach, inferring the movement of moisture through individual three-dimensional particle trajectories solved with differential equations. While Lagrangian models typically involves more complete physical mechanisms in particle dispersion processes, they exhibit substantially less numerical diffusion than Eulerian models, making them more adept at capturing small-scale atmospheric phenomena such as turbulence, convection, and dispersion, particularly over complex terrains (Wang et al., 2018; Tuinenburg and Staal, 2020). To date, several studies have employed both types of models, such as Eulerian and Lagrangian approaches with COSMO model (Winschall et al., 2014), Eulerian and Lagrangian frameworks in "UTrack-atmospheric-moisture" (Tuinenburg and Staal, 2020) , and WRF-WVT and FLEXPART-WRF (Cloux et al., 2021), to diagnose regional moisture sources and have conducted comparative analyses. However, these studies have not extensively explored the limitations of different model types and the causes of discrepancies between moisture tracking results. Moreover, the studies on the generation mechanisms of model uncertainties through the moisture tracking intercomparison is severely lacking.

Encompassing the world's highest plateau, the Tibetan Plateau (TP) region, often referred to as the "Asia water tower", has been experiencing a rapid retreat of glaciers and permafrost, accompanied by shifts in precipitation patterns and a pronounced warming trend in recent decades (Yao et al., 2018; Yao et al., 2022). Numerous research efforts based on meteorological analyses and climate proxy indicators (e.g., precipitation and ice-core isotopes) have comprehensively investigated into the hydrological cycle in this region (Yao et al., 2013; Yang et al., 2014; Liu et al., 2020b), while recent advancements in numerical moisture tracking models have further facilitated the quantitative analyses of moisture contribution to the TP (Chen et al., 2012; Li et al., 2022). We summarized the numerical moisture tracking studies over the TP in the last twenty years (Table 1), approximately one-fourth employed the Eulerian method, with the Water Accounting Model-2layers (WAM-2layers) being the predominant choice. The remaining three-fourths used the Lagrangian method, with the FLEXible PARTicle dispersion model (FLEXPART) and the "WaterSip" moisture source diagnostic method being the most widely applied. Existing studies predominantly utilize a singular methodology (either Eulerian or Lagrangian method), conducted over various study periods, across different regions in the TP, and with diverse forcing datasets. These

https://doi.org/10.5194/egusphere-2024-14
Preprint. Discussion started: 29 January 2024

diversities largely hinder the comprehensive comparison of the moisture tracking results based on different models and the attribution of their distinctions.

Table 1: Overview of Eulerian and Lagrangian moisture tracking studies in the TP and its vicinity.

	Model	Moisture source diagnosis	Study area	Forcing dataset	Study period	Reference
Eulerian	WAM-1layer	–	Central-western TP	ERA-I, NCEP-2	1979–2013	Zhang et al. (2017)
	WAM-2layers	–	Endorheic TP	ERA-I, MERRA-2, JRA-55	1979–2015	Li et al. (2019)
	WAM-2layers	–	Southern/northern TP	ERA-I	1979–2016	Zhang et al. (2019a)
	WAM-2layers	–	Major basins in TP	ERA-I, MERRA-2, JRA-55	1979–2015	Li et al. (2022)
	WAM-2layers	–	TP	ERA-I	1998–2018	Zhang (2020)
	CAM	–	Southern/northern TP	MERRA	1982–2014	Pan et al. (2018)
Lagrangian	FLEXPART	E–P	TP	NCEP-GFS	2005–2009 (summer)	Chen et al. (2012)
	FLEXPART	areal source–receptor attribution	Grassland on eastern TP	NCEP-CFSR	2000–2009	Sun and Wang (2014)
	FLEXPART	WaterSip	Four regions within TP	ERA-I	1979–2018 (May–August)	Chen et al. (2019)
	FLEXPART	areal source–receptor attribution	Xinjiang	NCEP-FNL	2008–2015 (April–September)	Zhou et al. (2019)
	FLEXPART	WaterSip	Southeastern TP	ERA-I	1980–2016 (June–September)	Yang et al. (2020)
	FLEXPART	WaterSip	Xinjiang	NCEP-CFSR	1979–2018	Yao et al. (2020)
	FLEXPART	WaterSip	Northern/Southern Xinjiang	NCEP-CFSR	1979–2018	Hu et al. (2021)
	FLEXPART	areal source–receptor attribution	Source region of Yellow River	NCEP-FNL	1979–2009	Liu et al. (2021)
	FLEXPART	WaterSip	Xinjiang	NCEP-CFSR	1979–2018 (April–September)	Yao et al. (2021)
	FLEXPART	E–P	Three-rivers headwater region	ERA-I	1980–2017 (boreal summer)	Zhao et al. (2021)
	FLEXPART	E–P	Three-rivers source region	NCEP-FNL	1989–2019	Liu et al. (2022)
	FLEXPART	WaterSip	Three-rivers headwater region	ERA-I	1980–2017	Zhao et al. (2023)
	HYSPLIT	WaterSip	Three-rivers headwater region	NNR1	1960–2017 (June–September)	Zhang et al. (2019b)
	HYSPLIT	E–P	Western TP	ERA-I	1979–2018 (winter)	Liu et al. (2020a)
	HYSPLIT	maximum specific humidity	Seven regions within TP	NCEP/NCAR	1961–2015 (summer extreme event)	Ma et al. (2020)
	HYSPLIT	contribution function and weighting	TP	NCEP-GDAS	1950–2015 (extreme precipitation events)	Ayantobo et al. (2022)
	HYSPLIT	WaterSip	Southern Xinjiang	ERA5	2021(June 15–17)	Chen et al. (2022)
	LAGRANTO	WaterSip	Southeastern TP	ERA-I	1979–2016 (winter extreme precipitation)	Huang et al. (2018)
	LAGRANTO	WaterSip	Three regions within TP	ERA-I	1979–2016 (winter extreme precipitation)	Qiu et al. (2019)
	LAGRANTO	WaterSip	Northern TP	ERA-I	2010–2018 (monsoon season)	Wang et al. (2023)
	QIBT	E and P	Southeastern TP	ERA-I	1982–2011 (April–September)	Xu and Gao (2019)

https://doi.org/10.5194/egusphere-2024-14
Preprint. Discussion started: 29 January 2024

Our thorough review of the different studies in Table 1 indicates potential inherent differences, such as the range of moisture sources and capability to capture specific precipitation events, in the application of the two types of numerical moisture tracing models across the TP. This prompts the questions: what are the potential differences in moisture tracking when using these two types of models, and what are the causes of these differences? In this study, we aim to compare the most commonly employed Eulerian and Lagrangian moisture tracking models in the TP region, namely WAM-2layers and FLEXPART-WaterSip (FLEXPART with "WaterSip" diagnostic method). Given that the TP's climate is predominantly shaped by the interactions between the Indian Summer Monsoon (ISM) and the mid-latitude westerlies, we have chosen an ISM-dominated basin (the Yarlung Zangbo River Basin, YB) and a westerlies-dominated basin (the upper Tarim River Basin, UTB) for our comparative analysis (Fig. S1). Section 2 provides detailed information on the foundational mechanisms, input data, and settings of the two models. Section 3 offers a comprehensive comparison of the simulations from the two models across both basins. Section 4 analyses the intermediate processes involved in moisture tracking in the two models, i.e., moisture fluxes in WAM-2layers and particle trajectories in FLEXPART. Section 5 further investigates the potential determinants of the observed disparities between models through a series of carefully designed numerical experiments. Overall, these comparisons and analyses are expected to serve as a reference for selecting and utilizing models, analyzing results, and correcting associated biases and errors in future studies on moisture tracking in the TP region.

2 Eulerian (WAM-2layers) and Lagrangian (FLEXPART-WaterSip) methods

The WAM-2layers V3.0.0b5 is adopted for the Eulerian moisture tracking in this study. The two-layers version, which is designed to deal with the wind shear in upper air, is an update to the previously used single-layer version (Van der Ent et al., 2010). As illustrated in the conceptual graphs (Fig. 1a), the underlying principle of WAM-2layers is the water balance equation (van der Ent et al., 2014):

$$\frac{\partial S_k}{\partial t} = \frac{\partial (S_k u)}{\partial x} + \frac{\partial (S_k v)}{\partial y} + E_k - P_k \pm F_v + \xi_k \quad (1)$$

where S_k is the atmospheric moisture content in layer k; t is time; u and v are wind fields in zonal (x) and meridional (y) directions; E and P are evaporation (occurs only in the bottom layer) and precipitation; F_v is the vertical moisture transport between the two layers; and ξ is the residual term. The model prescribes a two-layer division (~810 hPa with a standard surface pressure) and modifies F_v (with $4F_v$ in the net flux direction and $3F_v$ in the opposite direction) to consider turbulent moisture exchange.

https://doi.org/10.5194/egusphere-2024-14
Preprint. Discussion started: 29 January 2024

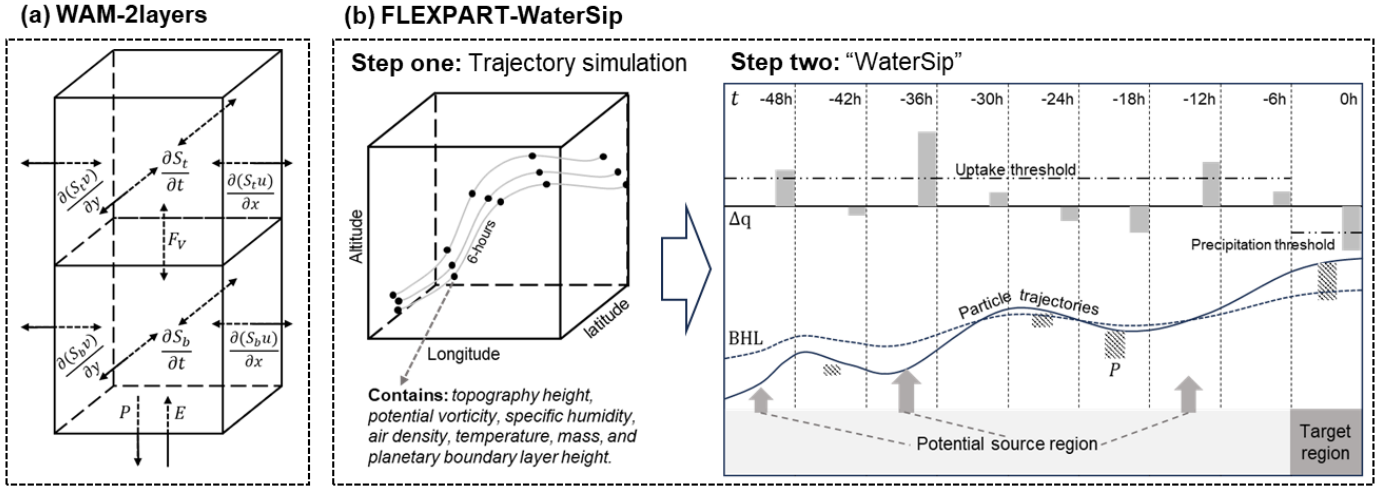

Figure 1: Mechanisms of WAM-2layers (a) and FLEXPART-WaterSip (b) method. "Step two" in (b) is adapted from Sodemann et al. (2008).

The Lagrangian particle trajectory simulation in this study is implemented using FLEXPART V10.4, a versatile model widely employed to simulate the transport and turbulent mixing of gases and aerosols in the atmosphere (Pisso et al., 2019). The domain-filling mode in FLEXPART adopts evenly distributed particles with equal mass to represent the entire atmosphere, offers a precise means to describe the global and regional atmospheric cycle at a theoretically infinitesimal spatial scale. In this study, five million particles were released from altitudes ranging from 100 m to 20000 m across the entire study region. The model output includes three-dimensional position, topography height, potential vorticity, specific humidity, air density, temperature, mass, and planetary boundary layer height (BLH) of each parcel at 6-hourly intervals (Fig. 1b). Similar to other Lagrangian models like HYSPLIT (Stein et al., 2016) and Lagranto (Sprenger and Wernli, 2015), FLEXPART on its own cannot identify potential moisture sources for precipitation in the target region or quantify their contributions. To address this limitation, the "WaterSip" method proposed by Sodemann et al. (2008) was adopted to identify potential moisture sources of the targeted moisture, mainly using humidity information along the particle trajectories simulated by FLEXPART. This method involves critical processing procedures (Fig. 1b) such as filtering trajectories that lead to precipitation, calculating specific humidity changes and their attributed fractions, and determining potential moisture sources based on moisture uptake thresholds as well as BLH. A more detailed methodology can be found in Sodemann et al. (2008). In summary, the FLEXPART-WaterSip moisture tracking method in this study intergrates the particle trajectory simulation using FLEXPART and the moisture source diagnostic procedure using "WaterSip".

Both WAM-2layers and FLEXPART-WaterSip are offline models that rely on meteorological fields as forcings. The fifth-generation atmospheric reanalysis product from the European Centre for Medium-Range Weather Forecasts (ERA5), which benefits from decades of advancements in data assimilation, core dynamics, and model physics (Hersbach et al., 2020), is

https://doi.org/10.5194/egusphere-2024-14
Preprint. Discussion started: 29 January 2024

used to drive both the WAM-2layers and FLEXPART-WaterSip models. The target time period for our simulations is July 2022, a month significantly influenced by the ISM in the TP region (Yao et al., 2013; Curio and Scherer, 2016). The entire moisture tracking domain spans 30°S–80°N and 40°W–140°E, covering nearly all potential oceanic and terrestrial source regions of the TP precipitation (Chen et al., 2012; Li et al., 2022). In both simulations, the YB and UTB areas are represented by gridded boundaries as shown in Fig. S1. Considering the number of particles released, data size, and computational resources needed, we use 1°×1° and 3-hourly ERA5 data to drive both models, although some specific variables used in the two models are different due to their distinct underlying physical mechanisms.

In WAM-2layers, targeted moisture is continuously released into Eulerian grids and tracked as it gradually accumulates and persistently diffuses between grids over time. The targeted moisture is released throughout the entire July (from 31-July to 1-July in the backward mode), and the backward tracking period extends to 1 June. A previous study in the TP reported that a period of ~30 days can ensure that around 95% of the tagged moisture returns to the ground (Zhang et al., 2017), which is also consistent with our numerical experiments in the YB and UTB (Fig. S2a). In comparison, FLEXPART-WaterSip model traces atmospheric particles released at each step independently, thereby avoiding interference between particles released at different times. This differs from WAM-2layers, where moisture released at different times converges into the same set of Eulerian grids. Consequently, scientists typically set the average residence time of moisture in the atmosphere (~10 days) as the moisture tracking period for a single release of particles in FLEXPART-WaterSip. To ensure a consistent tracking duration and maximize the tracking of the targeted moisture in both models (Fig. S2), the backward tracking time in FLEXPART-WaterSip was set to 30 days. For FLEXPART-WaterSip, although large deviations in actual air parcel movements may occur beyond the average residence time (~10 days), the increasing uncertainties in trajectories beyond this period are not expected to substantially affect the results, as the majority of moisture uptake occurs within 10 days (Sodemann et al., 2008). Our numerical experiments, as illustrated in Fig. S2b, indicate that within the first 10 days (20 days), we traced 89% (99%) of the precipitation moisture in the YB and 97% (99%) in the UTB.

3 Moisture tracking in two typical basins using Eulerian and Lagrangian methods

Figure 2 shows the simulated moisture sources of precipitation in July 2022 over the YB and UTB based on WAM-2layers and FLEXPART-WaterSip models. Moisture contributions are represented as equivalent water height (mm) over the source areas. In addition to significant local recycling, the moisture sources for YB precipitation primarily follow the ISM path, traversing the southern slope of the Himalayas, the Bay of Bengal (BB), the Indian subcontinent, and the Arabian Sea (AS), extending to the Southern Indian Ocean (SIO) (Figs. 2a and c). Meanwhile, the moisture sources for UTB precipitation mainly stretch along the westerlies to the Central Asia region (Figs. 2b and d). Spatially, notable disparities between the two models are most evident in the northwestern source region. Whether in the ISM-dominated YB or the westerlies-dominated UTB, FLEXPART-WaterSip, compared to WAM-2layers, exhibits only minimal moisture source contribution from the

https://doi.org/10.5194/egusphere-2024-14
Preprint. Discussion started: 29 January 2024

entire northwestern Eurasian continent and northeastern Atlantic. Another noteworthy detail is the clear north-eastward extension of moisture sources for UTB precipitation resolved by FLEXPART-WaterSip, reaching almost to the easternmost Tianshan Mountains (Fig. 2d), a feature absent in the results of WAM-2layers (Fig. 2b).

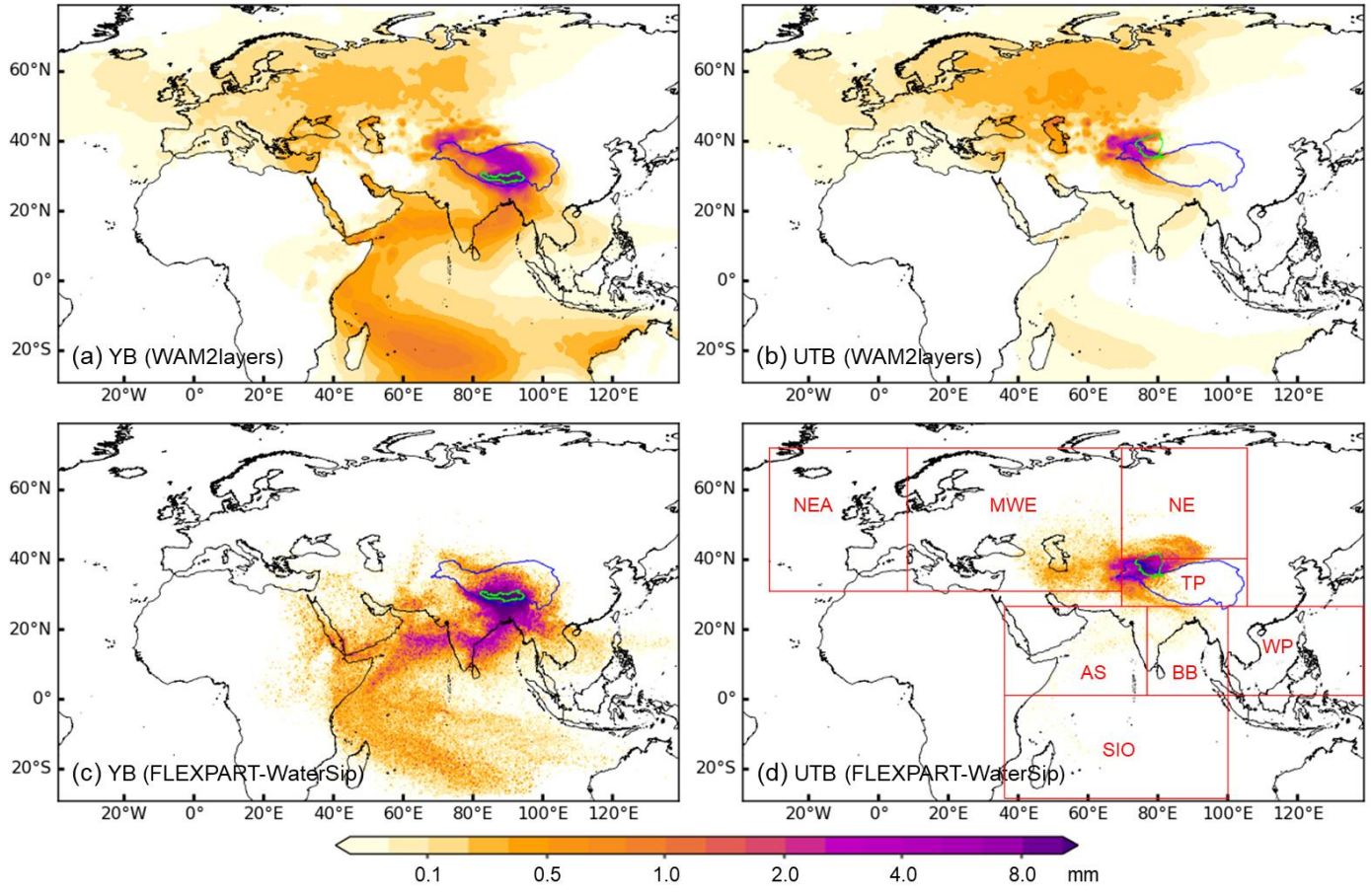

Figure 2: Spatial distributions of moisture contribution (equivalent water height over source areas) to precipitation in July 2022 in the YB (a and c) and UTB (b and d), simulated by WAM-2layers (a and b) and FLEXPART-WaterSip (c and d). Blue lines represent the TP boundary and cyan lines represent the boundaries of the two basins. Red boxes in (d) delineate the division of the eight source regions: North-eastern Atlantic (NEA), Midwestern Eurasia (MWE), Northern Eurasia (NE), TP, Arabian Sea (AS), Bay of Bengal (BB), Western Pacific (WP), and Southern Indian Ocean (SIO).

Figure 3 illustrates the differences in simulations based on the two models. When compared to FLEXPART-WaterSip, WAM-2layers tends to estimate higher moisture from the westerlies-dominated source regions for both basins. This extends from nearby sources (regions to the northwest of the YB and to the west of the UTB) to distant sources across the entire northwestern Eurasian continent and northeastern Atlantic. Additionally, WAM-2layers estimates higher moisture

https://doi.org/10.5194/egusphere-2024-14
Preprint. Discussion started: 29 January 2024

contribution from large parts of the Indian Ocean, particularly the distant SIO in the YB simulation. In contrast, lower contributions estimated by WAM-2layers mainly occur in local and nearby source regions located opposite to the westerlies direction. Notably, around the Red Sea and Persian Gulf regions, WAM-2layers simulations estimate lower moisture contribution in exhibit an underestimation of moisture contribution in certain scattered areas compared to FLEXPART-WaterSip, especially in the YB simulation (Fig. 3a). These disparities between the two models remain consistent in both absolute and relative terms (Figs. 3 and S3).

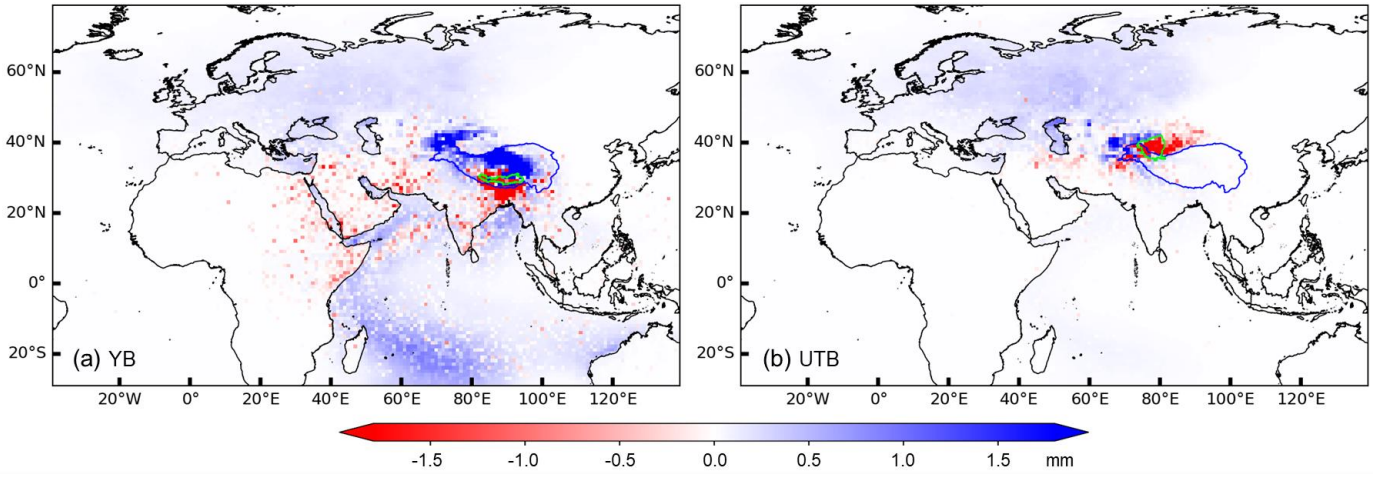

Figure 3: Absolute differences in moisture contributions between the two simulations (WAM-2layers minus FLEXPART-WaterSip) for the YB (a) and UTB (b).

Considering the distribution of moisture sources, eight critical source regions (as indicated by red boxes in Fig. 2d) are selected for further quantitative analysis. Figure 4 shows the relative contributions from these eight moisture source regions to YB and UTB precipitation. Both models indicate that the major moisture sources for the YB are local recycling and ISM regions (TP, AS, BB, and SIO), whereas for the UTB, the primary sources are local recycling and westerly regions (TP, NE, and MWE). For moisture contribution from the TP to the YB, WAM-2layers estimates it at 35%, which is about two-thirds of the estimate by FLEXPART-WaterSip (52%). Even more substantial difference is observed for the estimated TP's contribution to the UTB: the relative contributions from TP are estimated to be 24% by WAM-2layers but 68% by FLEXPART-WaterSip. For distant sources, the SIO is the most representative one for the YB, with WAM-2layers estimating its contribution at 26% (cf. 10% for FLEXPART-WaterSip). Meanwhile, for the MWE, the most representative distant source of the UTB, WAM-2layers estimates a contribution (44%) even triple that calculated by FLEXPART-WaterSip (13%). In addition to the disparities showcased in Figs. 2 and 3, Fig. 4 quantitatively reveals that the differences between these two sets of simulations are considerably larger for the UTB than for the YB.

https://doi.org/10.5194/egusphere-2024-14
Preprint. Discussion started: 29 January 2024

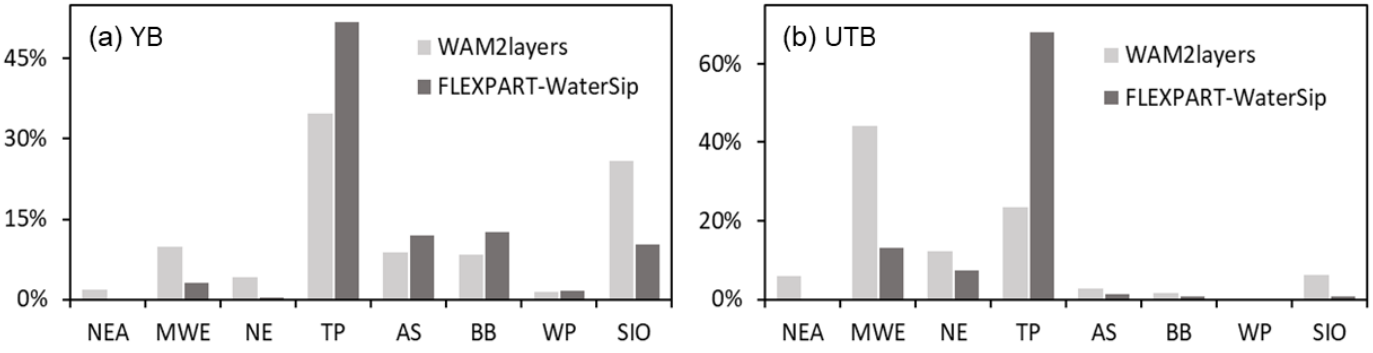

Figure 4: Relative moisture contributions (%) to precipitation over the YB (a) and UTB (b) from the eight source regions (NEA, MWE, NE, TP, AS, BB, WP, and SIO), simulated by WAM-2layers and FLEXPART-WaterSip.

To further evaluate potential disparities between the two models, we specifically identified a day with maximum precipitation in July, representing an instance of extreme precipitation events, for additional moisture tracking simulations. Based on the daily precipitation time series of the two basins (Fig. S4), the extreme precipitation events in YB and UTB occurred on 21-July and 14-July, respectively. Figure S5 shows the simulated moisture sources of these two events using WAM-2layers and FLEXPART-WaterSip, while Figs. S6 and S7 show the spatial and regional differences between the two simulations (WAM-2layers minus FLEXPART-WaterSip). In addition to differences in absolute contribution amounts, the spatial distributions of moisture sources and the spatial differences between the two models for these extreme events in the YB and UTB are generally consistent with those for the entire July (Figs. S5–6; cf. Figs. 2–3). Meanwhile, the relative contributions from the eight selected sources in Fig. S7 closely match those in Fig. 4. In general, simulation disparities between the two models are less pronounced in the ISM-dominated YB than in the westerlies-dominated UTB. The most notable characteristic of WAM-2layers, as compared to FLEXPART-WaterSip, is that it tends to estimate higher moisture contribution from the westerlies-dominated sources and distant sources but lower contribution from local recycling and nearby sources opposite to the westerlies direction.

4 Moisture fluxes in Eulerian method and particle trajectories in Lagrangian method

When tracing moisture sources, WAM-2layers primarily utilizes horizontal moisture fluxes in the upper and lower layers (divided at ~810 hPa at a standard surface pressure; see Fig. 1a) to determine the backward transport of water vapor from the target region to global sources. The average moisture transport fluxes in the two layers during the entire simulation period estimated by WAM-2layers are shown in Fig. 5. The ISM-dominated moisture transport to the TP region primarily occurs in the lower layer, whereas the westerlies-dominated moisture transport to the region is mainly from the north in the lower layer and from the west in the upper layer, a phenomenon pronounced in the northwest vicinity of the UTB.

https://doi.org/10.5194/egusphere-2024-14
Preprint. Discussion started: 29 January 2024

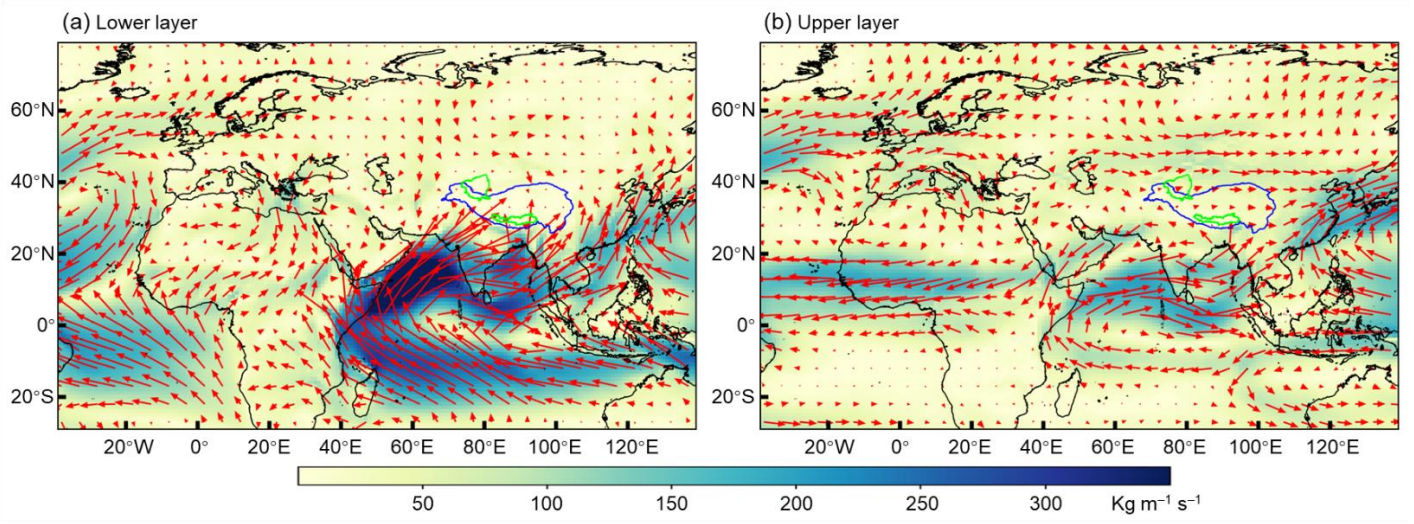

Figure 5: Average moisture transport fluxes (kg m^{-1} s^{-1}) in the lower (a) and upper (b) layers in the WAM-2layers during the entire simulation period.

In comparison, FLEXPART outputs extensive information on air particles and trajectories, providing valuable insights into diagnosing moisture sources. Figure 6 shows the spatial distributions of particles and trajectories that bring moisture to precipitation over the YB and UTB in the FLEXPART-WaterSip simulation. It should be noted that the particles and trajectories in Fig. 6 are clustered using the K-means method for clearer graphical representation (number of particles reduced by a factor of 100, and number of trajectories by a factor of 150), which may have filtered out some chaotic and distant particles and trajectories. Particles released from the YB predominantly travel south-westward, whereas those from the UTB primarily spread westward. Within about 15 days, the traced particles can transport from target regions to the farthest end of the source regions. As suggested by the results of backward tracking days, there are approximately three distinct fastest moisture transport paths to the YB (red arrows in Fig. 6a), while the most pronounced moisture transport path to the UTB is confined to western routes (red arrow in Fig. 6b).

https://doi.org/10.5194/egusphere-2024-14
Preprint. Discussion started: 29 January 2024

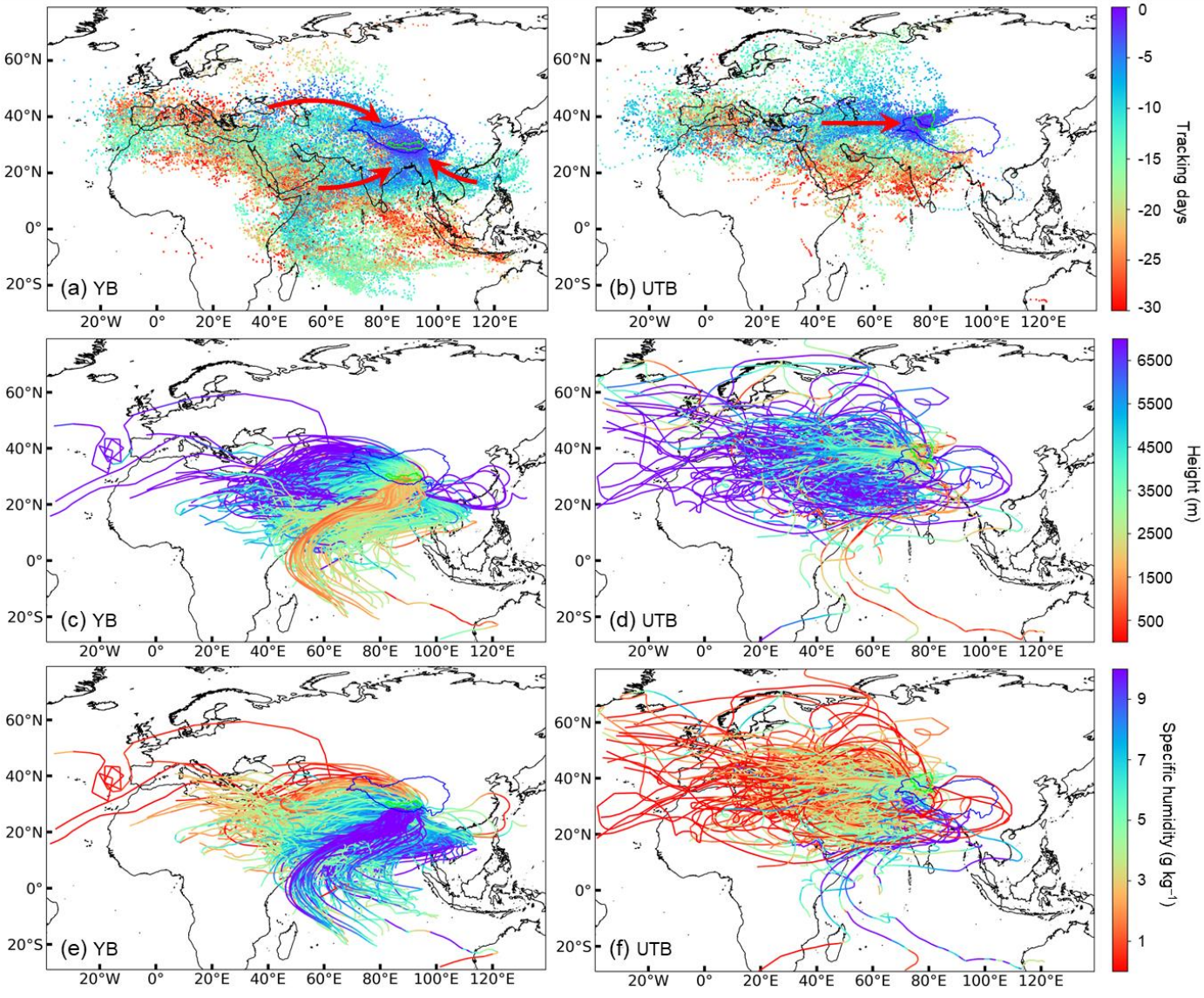

Figure 6: Spatial distributions of particles (a and b) and trajectories (c–h) that bring moisture to precipitation over the YB (a, c, and e) and UTB (b, d, and f), as simulated by FLEXPART. (a and b) are particles color-coded by backward-tracking days (0–30 days). (c and d) are trajectories color-coded by height (m, above ground) at each numerical step. (e and f) are trajectories color-coded by specific humidity (g kg^{-1}) at each numerical step.

Another notable observation is the rapid north-eastward transport of tracked particles in the UTB over a short period (Fig. 6b), a phenomenon challenging to discern in the WAM-2layers simulations (Figs. 2b and d) and its two-layer moisture transport fluxes (Fig. 5). This suggests the capability of FLEXPART model to capture smaller scale atmospheric processes that may not be as apparent in the Eulerian model. Upon closer examination of the vertical wind patterns at 700 hPa and 300

https://doi.org/10.5194/egusphere-2024-14
Preprint. Discussion started: 29 January 2024

hPa across the study domain (Fig. 7), we observed more complex and variable convective activities near the UTB compared to those around the YB. This further implies that the modelling capability of WAM-2layers for moisture sources of the UTB may be less robust than for the YB, consistent with the observation that the simulation disparities between the two models are more pronounced in the UTB than that in the YB (Fig. 4). The vertical wind patterns in Fig. 7 also explain another phenomenon around the Red Sea and Persian Gulf regions. The spatial distributions of moisture sources simulated by WAM-2layers show a consistent alignment with the land–sea boundaries (see Figs. 2a–b and Figs. S5a–b). This corresponds with the common understanding that greater evaporation (over oceans) means a higher potential for moisture contribution to the target region. However, in FLEXPART-WaterSip simulations, terrestrial sources with high moisture contributions are widely distributed around the Red Sea and Persian Gulf (Figs. 2c–d), accompanied by enhanced upward motion compared to the adjacent oceanic regions (Fig. 7). Essentially, FLEXPART-WaterSip detects only the increases in specific humidity, possibly in the mid-to-upper atmosphere caused by strong land convection, while the actual sources of these increased moisture might still be the strong evaporation from oceans. In this regard, the estimation from WAM2-layers is more reasonable than that from FLEXPART-WaterSip.

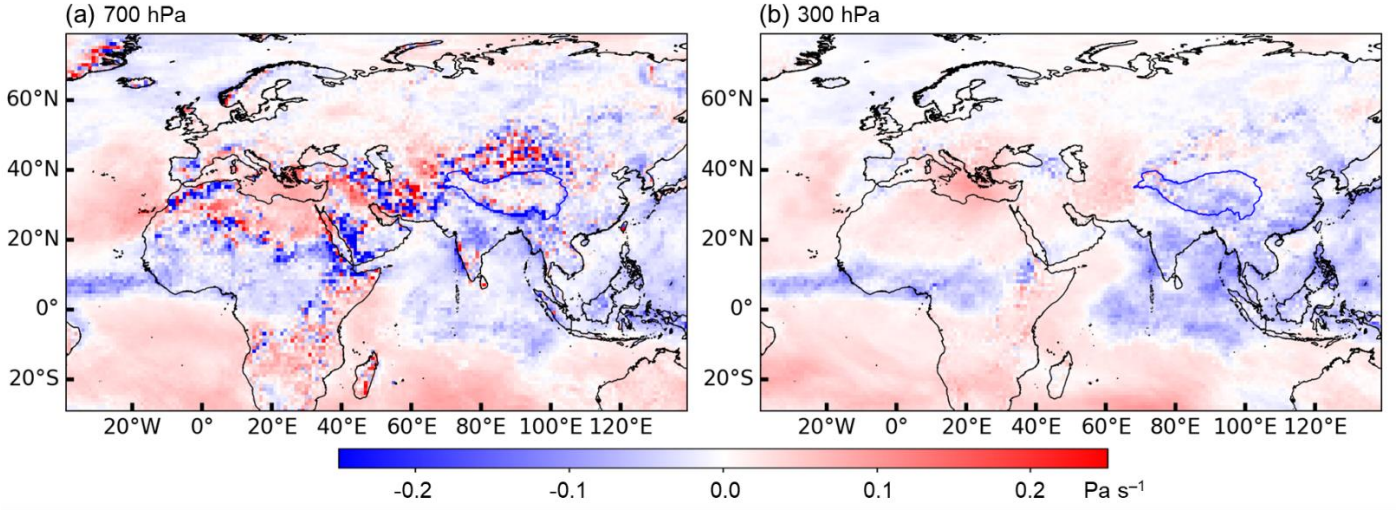

Figure 7: Atmospheric vertical velocities (Pa s^{-1}) at 700 hPa and 300 hPa across the entire study domain. Note the negative values indicate upward motion (ascent).

In terms of trajectories in Figs. 6c–d, those originating from the western sources are mainly at higher altitudes (even exceeding 6000 m) but undergo a notable descent in altitude before reaching the target region, forming a strip-like lower atmospheric transport channel in the western part of the target region. Considering the horizontal moisture transport in WAM-2layers, the upper layer moisture originating from the northwestern Eurasian is also higher than that in the lower layer (Fig. 5). For trajectories from the ISM-dominated sources, they are at relatively lower altitudes, with some originating from the SIO even descending below 1000 m. Generally, the moisture-carrying capacity of these trajectories correlates with both

https://doi.org/10.5194/egusphere-2024-14
Preprint. Discussion started: 29 January 2024

their altitude and moisture conditions in the source regions. In conjunction with Figs. 6e–f, trajectories originating from the ISM-dominated regions and lower altitudes exhibit higher moisture content, whereas those from the westerlies-dominated regions and higher altitudes are characterized by lower moisture content.

A notable difference between WAM-2layers and FLEXPART-WaterSip, as highlighted in Fig. 2, is that FLEXPART-WaterSip model fails to capture most moisture source regions across the entire northwestern Eurasia for both basins when compared to WAM-2layers. Specifically, particle trajectories simulated by FLEXPART (see Fig. 6) are only sparsely distributed across northwestern Eurasia, particularly for the YB. This inconsistency is also evident when comparing results from previous studies using WAM-2layers (Zhang et al., 2017; Li et al., 2022) and FLEXPART-WaterSip (Chen et al., 2019; Yao et al., 2020). This indicates that the underestimated moisture contribution from the westerlies-dominated northwestern Eurasia in FLEXPART-WaterSip, as compared to WAM-2layers, is largely attributed to a reduced proportion of air particles from this region reaching the target region.

5 Potential determinants of disparities in moisture tracking based on Eulerian and Lagrangian methods

We now turn to a more comprehensive and in-depth examination of the disparities observed in Sections 3 and 4. Considering the underlying physics of the models, forcing datasets, parameter selections, and our computational capabilities, we designed three numerical experiments to examine potential factors influencing the disparities in simulations based on WAM-2layers and FLEXPART-WaterSip.

Experiment 1 – model resolution: The simulation of moisture sources by WAM-2layers is essentially a dynamic reproduction of moisture transport conditions from forcing datasets, which means that the simulation accuracy heavily depends on the spatial-temporal resolution of input data. In this numerical experiment, we replace the 1°×1° and 3-hourly forcing data with 0.25°×0.25° and hourly ERA5 data to examine whether improved forcing dataset resolutions contribute to more detailed moisture source attributions. Particularly, we examine whether this change would impact the higher moisture contribution from distant source regions estimated by WAM-2layers. Results of this experiment are summarized in Fig. S8.

Experiment 2 – number of particles: Employing a source diagnostic methodology based on particle trajectories inevitably confines the identified moisture sources to these trajectories. Therefore, a lower number of trajectories may result in potential inaccuracies when representing small to medium-scale atmospheric processes. We are interested in understanding whether the relatively sparse particle trajectories over distant source regions would introduce substantial uncertainties when estimating moisture contributions in FLEXPART-WaterSip. In this numerical experiment, we decrease the number of particles initially released in FLEXPART from five million to one million. Results of this experiment are summarized in Fig. S9.

https://doi.org/10.5194/egusphere-2024-14
Preprint. Discussion started: 29 January 2024

Experiment 3 – moisture source diagnosis: Different from the "WaterSip" method proposed by Sodemann et al. (2008), which attributes precipitation at a specific point within the target region to moisture uptake from multiple points along the trajectories, Sun and Wang (2014) introduced the "areal source–receptor attribution" method, focusing on a regional rather than a point scale. The "areal source–receptor attribution" method aims to calculate the total moisture contribution from an examined source to precipitation over the entire target region, as opposed to specific points. This method allows for distinguishing moisture contributions from within and outside the examined sources along the trajectories (see Sun and Wang (2014) for detailed methodology). In this numerical experiment, we utilize "areal source–receptor attribution" method to quantify moisture contributions from the eight source regions.

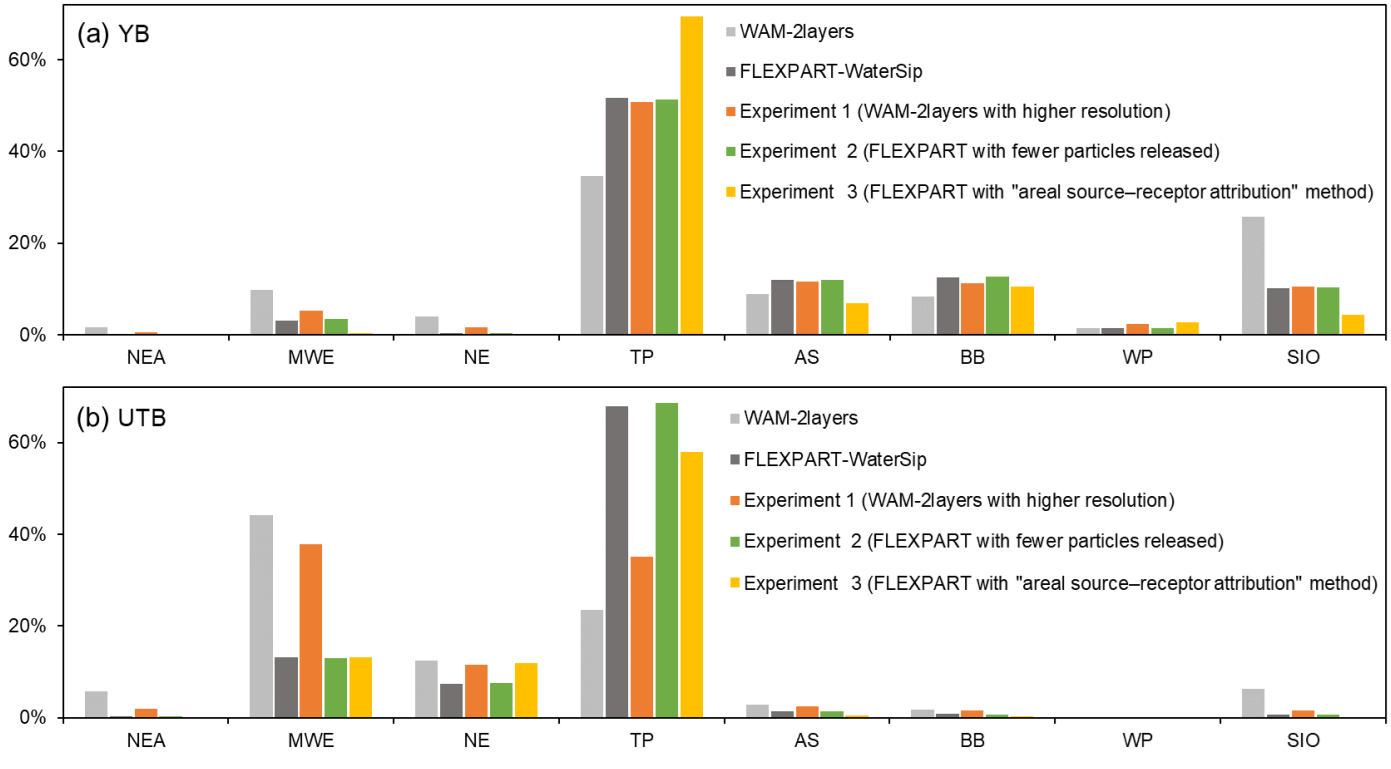

Figure 8: Relative moisture contributions (%) to precipitation over the YB (a) and UTB (b) from the eight source regions, simulated by the original WAM-2layers and FLEXPART-WaterSip methods and the three numerical experiments.

Figure 8 shows the relative moisture contributions of the eight source regions to the YB and UTB in three numerical experiments and the original simulations from both models (as in Sections 3 and 4). In Experiment 1, increasing the spatial-temporal resolution of forcing dataset has brought the WAM-2layers simulations closer to the original FLEXPART-WaterSip simulations, particularly in the YB. The moisture contribution from TP to the YB (UTB) increases from 35% (24%) to 51% (35%). For distant source regions, the moisture contributions from the MWE and SIO to the YB (UTB) decrease

https://doi.org/10.5194/egusphere-2024-14
Preprint. Discussion started: 29 January 2024

from 10% (44%) to 5% (38%) and from 26% (6%) to 11% (2%), respectively. A closer inspection of the spatial differences between Experiment 1 and original WAM-2layers simulations (Fig. 9) reveals that increasing model resolutions effectively reduces moisture contributions from distant source regions for both basins. However, this experiment fails to distinguish between simultaneous overestimation and underestimation in source regions around the two basins; instead, it results in enhanced moisture contributions from local and nearby sources. Results from Experiment 2 closely resemble the original FLEXPART-WaterSip simulation (Figs. 8, S9, and S10), yet reducing the number of released particles limits our ability to discern finer details in the spatial distribution of moisture sources (Fig. S9). In Experiment 3, the "areal source–receptor attribution" method, when compared to the original FLEXPART-WaterSip simulation, estimates reduced TP moisture contribution to the UTB but enhanced contribution for the YB. In contrast to the "WaterSip" method, the "areal source–receptor attribution" method utilizes all simulated trajectories for moisture source diagnoses, which may accumulate errors in trajectories that do not lead to precipitation in the target region. Reapplying the "areal source–receptor attribution" method with trajectories filtered by the "WaterSip" method can produce moisture contributions that align more closely with the original FLEXPART-WaterSip estimation (results not shown).

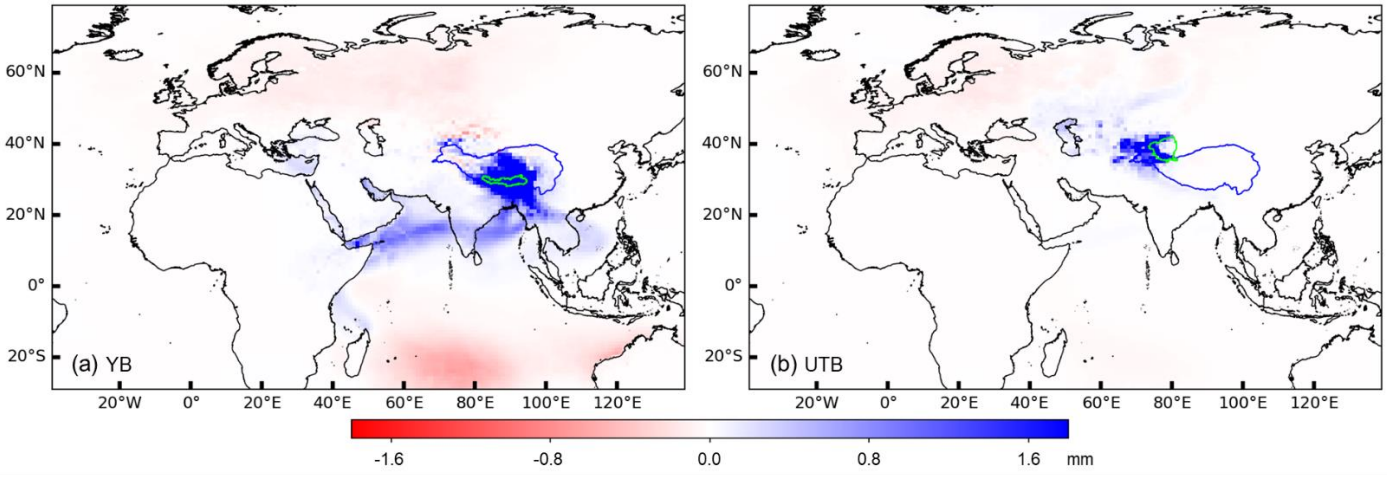

Figure 9: Absolute differences in moisture contributions between Experiment 1 and original WAM-2layers simulations (Experiment 1 minus original WAM-2layers) for the YB (a) and UTB (b).

Another crucial consideration is whether the information embedded in Lagrangian particles can adequately capture the impact of surface evaporation over the source regions. For example, intense tropical convection continuously lifts lower atmospheric moisture to upper levels and forms precipitation, while strong surface evaporation consistently replenishes moisture to the lower atmosphere. During this process, even though substantial evaporation enters the lower atmosphere, it may not be fully reflected by changes in specific humidity. Additionally, evaporation primarily occurs at the surface, while precipitation moisture condensation mainly happens in the mid-to-upper atmosphere. Therefore, changes in specific humidity in the lower atmosphere may not effectively capture the moisture loss associated with upper-level precipitation. In

https://doi.org/10.5194/egusphere-2024-14
Preprint. Discussion started: 29 January 2024

this context, we randomly selected one trajectory from the SIO leading to precipitation in the YB and another from the NEA responsible for precipitation in the UTB (Fig. S11). Leveraging the high spatial-temporal resolution ERA5 data, we then conducted a comprehensive analysis based on these two trajectories.

Figure 10 illustrates the 6-hourly time series of particle heights (m), 1.5 BLH (m), specific humidity changes (g kg^{-1} $6h^{-1}$), vertical velocities in 700 hPa (Pa s^{-1}), precipitation (mm), and evaporation (mm) along the two selected trajectories, with the last three variables extracted from the 0.25°×0.25° and 6-hourly ERA5 dataset. Figure 10 clearly shows the acquisition of moisture in the source regions and subsequent loss upon reaching the target regions (specific humidity changes), pronounced updrafts during monsoonal moisture transport (vertical velocity in Fig. 10a), weak convective activities over the hinterland Eurasia (vertical velocity in Fig. 10b), strong evaporation and precipitation in the ISM-dominated regions (precipitation and evaporation in Fig. 10a), and weak precipitation but strong diurnal evaporation in the westerlies-dominated regions (precipitation and evaporation in Fig. 10b).

We then select six time periods (shaded areas in Fig. 10) for detailed analysis. Relative to Period 1, Period 2 exhibits less moisture loss but stronger convective activities and enhanced precipitation. During period 3, intense atmospheric subsidence is observed, suggesting that evaporation may struggle to transport to the upper atmosphere. Nonetheless, moisture uptake during this period does not show a noticeable reduction. Contrary to Period 4, Period 5 experiences more intense precipitation but is characterized by moisture uptake. During Period 6, minimal evaporation and relatively weak atmospheric subsidence occur, yet the moisture uptake remains comparable to other periods. It should be noted that the comparisons here may involve substantial uncertainties and can be potentially influenced by various meteorological factors. In fact, using specific humidity changes to assess evaporation, precipitation, and moisture transport over source regions still remains challenging. Actually, the “WaterSip” method have already employs a threshold of 1.5 BLH and 0.2 g^{-1} kg^{-1} $6h^{-1}$ for specific humidity changes to filter out a considerable number of potential erroneous trajectories over the source regions. Specifically, Keune et al. (2022) explored the biases in the “WaterSip” method induced by various threshold settings and introduced an initial framework for diagnosis, attribution, and correction using averaged evaporation and precipitation over the source and sink regions. This further suggests that the current method of diagnosing moisture sources around the TP based on particle trajectories still holds substantial potential for improvement and refinement.

https://doi.org/10.5194/egusphere-2024-14
Preprint. Discussion started: 29 January 2024

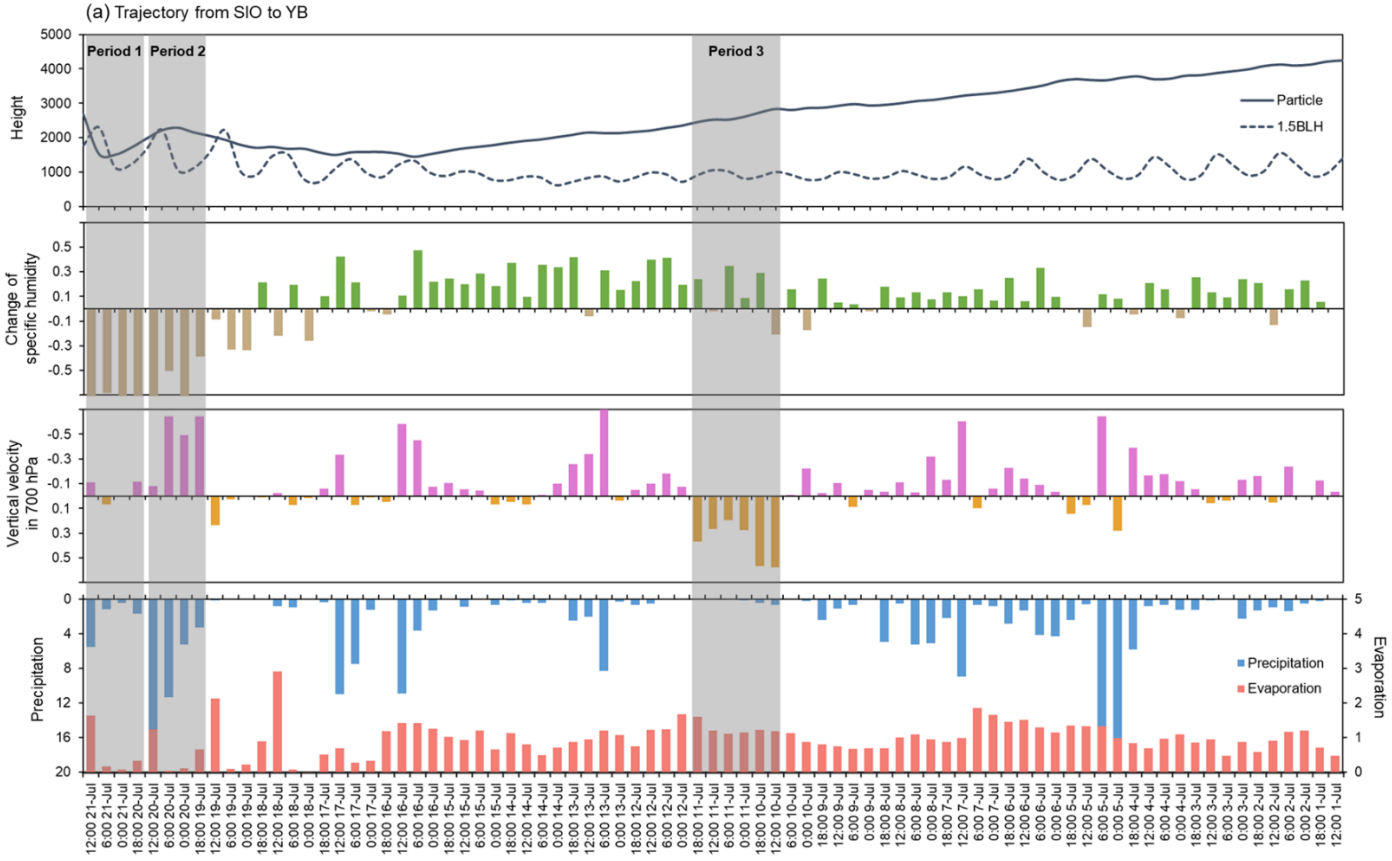

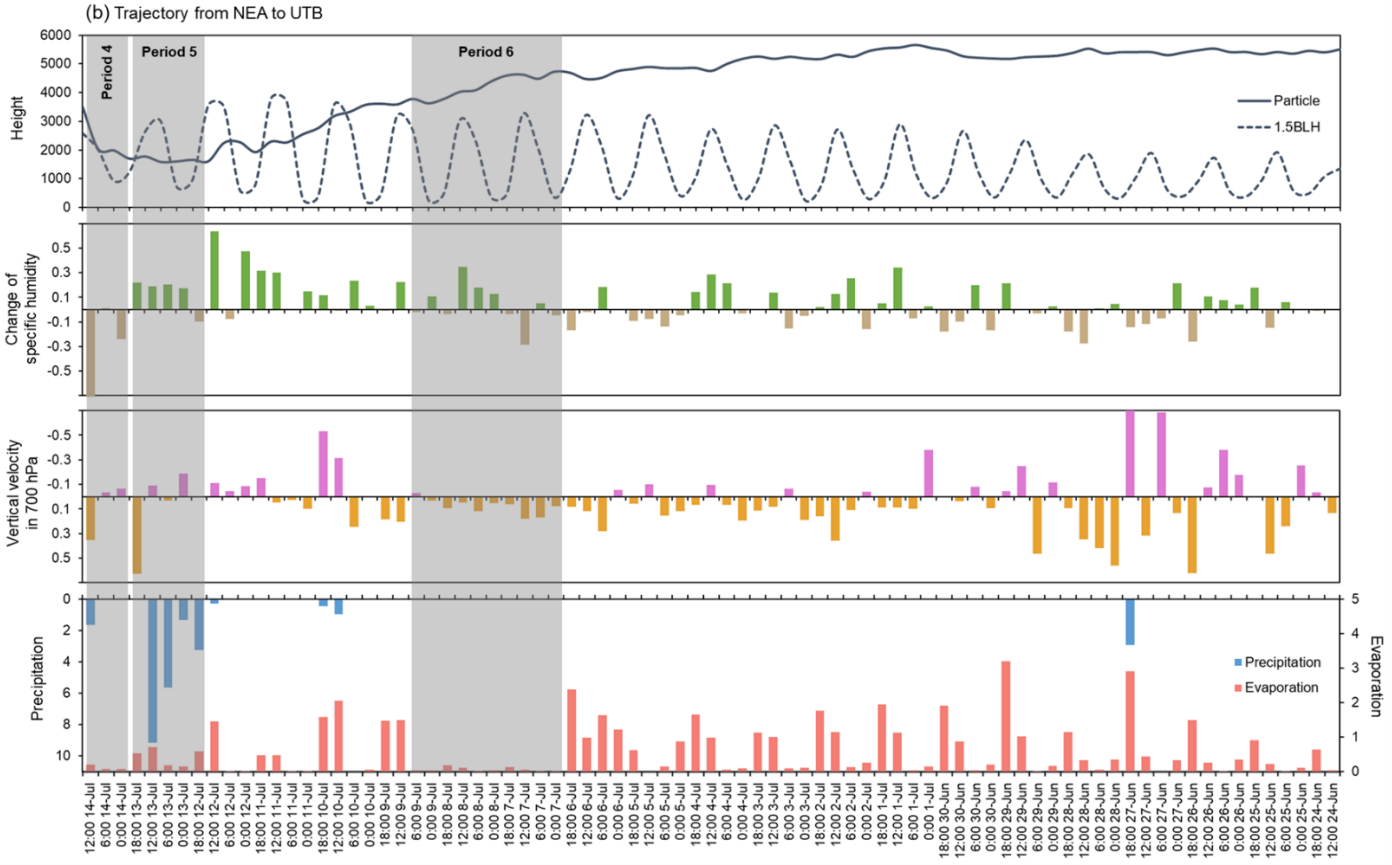

https://doi.org/10.5194/egusphere-2024-14
Preprint. Discussion started: 29 January 2024

Figure 10: Time series of particle heights, 1.5 BLH, specific humidity changes, vertical velocities in 700 hPa, precipitation, and evaporation on 6-hourly interval in the selected trajectories from SIO to YB during 12:00 21-July and 12:00 1-July (a) and from NEA to UTB during 12:00 14-July and 12:00 24-June (b). Note that the time series is in reverse order.

6 Discussions and conclusions

Over the past few decades, considerable efforts have been directed towards identifying and quantifying the contributions of moisture sources to precipitation over the TP. A synthesis of these studies reveals that the most commonly used Eulerian and Lagrangian moisture tracking models are WAM-2layers and FLEXPART-WaterSip, respectively. However, the suitability of these models, which incorporate differing physical mechanisms, for the TP has not yet been thoroughly examined. To address this gap, this study focused on two representative basins surrounding the TP: the YB (representing the ISM-dominated regions) and the UTB (representing the westerlies-dominated regions). Moisture source contributions to precipitation over these two basins were tracked employing the WAM-2layers and FLEXPART-WaterSip models. We then investigated the differences in the moisture tracking results of these two methods in the two basins and discussed their potential determinants.

WAM-2layers model, designed for moisture tracking based on the water balance equation at a spatial-temporal resolution constrained by the forcing dataset, faces challenges in accurately capturing moisture transport to target regions through smaller-scale atmospheric phenomenon such as turbulence and convection. Its effectiveness in regions with complex weather conditions is generally inferior to that of FLEXPART-WaterSip when operating with forcing datasets of the same resolution. For instance, over the UTB that is characterized by substantial spatial heterogeneity in local convective activities, WAM-2layers struggles to identify the moisture transported from source regions to the northeast of the basin. Moreover, disparities in simulations between the two models are less pronounced in the ISM-dominated YB compared to the westerlies-dominated UTB. In this context, WAM-2layers, compared to FLEXPART-WaterSip, tend to estimate higher moisture contributions from westerlies-dominated and distant source regions but lower contributions from local and nearby source regions opposite to the westerlies direction. However, these issues can be mitigated by utilizing a higher spatial-temporal resolution forcing dataset in WAM-2layers, particularly in the YB region. This approach helps alleviate the potential overestimation from distant sources and underestimation from local recycling for both basins, although it is less effective in correcting the potential overestimation from nearby westerlies-dominated sources. Despite these challenges, a key advantage of WAM-2layers is its inherent ability to distinguish between moisture from evaporation and precipitation, making it more adept at capturing variations in moisture source contributions arising from different surface evaporation. For instance, in regions surrounding the Red Sea and Persian Gulf regions, FLEXPART-WaterSip primarily detects changes in atmospheric humidity due to intense convection, mainly occurring in the adjacent terrestrial regions, whereas WAM-2layers identifies significantly stronger evaporation from oceans.

https://doi.org/10.5194/egusphere-2024-14
Preprint. Discussion started: 29 January 2024

The FLEXPART model is designed to simulate air particles based on a well-established set of physical mechanisms, which enables accurate representation of the three-dimensional movement of particles in the atmosphere. However, the subsequent process of "WaterSip" in diagnosing moisture sources using information from simulated trajectories may potentially introduce additional errors. For instance, matching the information on particles' specific humidity with moisture uptake from evaporation and moisture loss from precipitation is always challenging. Nevertheless, compared to WAM-2layers, FLEXPART-WaterSip offers a precise depiction of the three-dimensional distribution of moisture sources, especially in capturing smaller-scale convective systems with high spatial heterogeneity.

This study provides valuable reference and guidance for future numerical simulations focusing on tracking moisture sources in the TP region, including multiple aspects such as model selection, the accuracy of forcing data, error and uncertainty analysis, and potential strategies for improving simulate accuracy. While recognizing that each model has its most suitable application scenarios, this paper underscores the importance of considering differences between models and potential uncertainties in moisture tracking results. Although the current findings are limited to short-term simulations in selected regions, our future work aims to extend to larger and more refined spatial-temporal scales and to explore the feasibility of employing more advanced techniques for moisture source identification in both Eulerian and Lagrangian frameworks.

Code availability. The official website of WAM-2layers is: https://wam2layers.readthedocs.io/en/latest/. The official website of FLEXPART is: https://www.flexpart.eu/. For the WaterSip method, the authoritative website is: https://wiki.app.uib.no/gfi/index.php?title=WaterSip. All the original codes are available from these official websites.

Data availability. ERA5 data are available at the Climate Data Store (CDS) (https://cds.climate.copernicus.eu/).

Author contributions. YL conceptualized the study, carried out numerical simulations, conducted formal analysis, prepared figures and wrote the initial draft. CW contributed to the editing, discussion, and interpretation. QT, SY, and BS provided comments on the manuscript. HP and SX provided supervision during the simulations and writing.

Competing interests. The contact author has declared that neither they nor their co-authors have any competing interests.

Financial support. This work was financially supported by the Second Tibetan Plateau Scientific Expedition and Research Program (grant no. 2019QZKK0207-02) and the Natural Science Foundation of Hubei Province of China (grant no. 2022CFB785).

https://doi.org/10.5194/egusphere-2024-14
Preprint. Discussion started: 29 January 2024

References

Ayantobo, O.O., Wei, J., Hou, M., Xu, J., Wang, G.: Characterizing potential sources and transport pathways of intense moisture during extreme precipitation events over the Tibetan Plateau, J. Hydrol. 615, 128734, https://doi.org/10.1016/j.jhydrol.2022.128734, 2022

Chen, B., Xu, X.D., Yang, S., Zhang, W.: On the origin and destination of atmospheric moisture and air mass over the Tibetan Plateau, Theor. Appl. Climatol. 110, 423-435, https://doi.org/10.1007/s00704-012-0641-y, 2012

Chen, B., Zhang, W., Yang, S., Xu, X.D.: Identifying and contrasting the sources of the water vapor reaching the subregions of the Tibetan Plateau during the wet season, Climate Dyn. 53, 6891-6907, https://doi.org/10.1007/s00382-019-04963-2, 2019

Chen, Y., Liu, B., Cai, X., Zhou, T., He, Q.: Moisture transport and sources of an extreme rainfall event of June 2021 in southern Xinjiang, China, Adv. Clim. Change Res. 13, 843-850, https://doi.org/10.1016/j.accre.2022.11.010, 2022

Cloux, S., Garaboa-Paz, D., Insua-Costa, D., Miguez-Macho, G., Pérez-Muñuzuri, V.: Extreme precipitation events in the Mediterranean area: contrasting two different models for moisture source identification, Hydrol. Earth Syst. Sci. 25, 6465-6477, https://doi.org/10.5194/hess-25-6465-2021, 2021

Curio, J., Scherer, D.: Seasonality and spatial variability of dynamic precipitation controls on the Tibetan Plateau, Earth Syst. Dynam. 7, 767-782, https://doi.org/10.5194/esd-7-767-2016, 2016

Gimeno, L., Stohl, A., Trigo, R.M., Dominguez, F., Yoshimura, K., Yu, L., Drumond, A., Durán-Quesada, A.M., Nieto, R.: Oceanic and terrestrial sources of continental precipitation, Rev. Geophys. 50, RG4003, https://doi.org/10.1029/2012RG000389, 2012

Gimeno, L., Vazquez, M., Eiras-Barca, J., Sori, R., Stojanovic, M., Algarra, I., Nieto, R., Ramos, A.M., Duran-Quesada, A.M., Dominguez, F.: Recent progress on the sources of continental precipitation as revealed by moisture transport analysis, Earth-Sci. Rev. 201, 103070, https://doi.org/10.1016/j.earscirev.2019.103070, 2020

Hersbach, H., Bell, B., Berrisford, P., Hirahara, S., Horanyi, A., Munoz-Sabater, J., Nicolas, J., Peubey, C., Radu, R., Schepers, D., Simmons, A., Soci, C., Abdalla, S., Abellan, X., Balsamo, G., Bechtold, P., Biavati, G., Bidlot, J., Bonavita, M., De Chiara, G., Dahlgren, P., Dee, D., Diamantakis, M., Dragani, R., Flemming, J., Forbes, R., Fuentes, M., Geer, A., Haimberger, L., Healy, S., Hogan, R.J., Holm, E., Janiskova, M., Keeley, S., Laloyaux, P., Lopez, P., Lupu, C., Radnoti, G., de Rosnay, P., Rozum, I., Vamborg, F., Villaume, S., Thepaut, J.-N.: The ERA5 global reanalysis, Quart. J. Roy. Meteorol. Soc. 146, 1999-2049, https://doi.org/10.1002/qj.3803, 2020

Hu, Q., Zhao, Y., Huang, A., Ma, P., Ming, J.: Moisture Transport and Sources of the Extreme Precipitation Over Northern and Southern Xinjiang in the Summer Half-Year During 1979–2018, Frontiers in Earth Science 9, https://doi.org/10.3389/feart.2021.770877, 2021

Huang, W., Qiu, T., Yang, Z., Lin, D., Wright, J.S., Wang, B., He, X.: On the formation mechanism for wintertime extreme precipitation events over the southeastern Tibetan Plateau, J. Geophys. Res.-Atmos. 123, 12,692-612,714, https://doi.org/10.1029/2018JD028921, 2018

Keune, J., Schumacher, D.L., Miralles, D.G.: A unified framework to estimate the origins of atmospheric moisture and heat using Lagrangian models, Geosci. Model Dev. 15, 1875-1898, https://doi.org/10.5194/gmd-15-1875-2022, 2022

Li, Y., Su, F., Chen, D., Tang, Q.: Atmospheric Water Transport to the Endorheic Tibetan Plateau and Its Effect on the Hydrological Status in the Region, J. Geophys. Res.-Atmos. 124, 12864-12881, https://doi.org/10.1029/2019jd031297, 2019

Li, Y., Su, F., Tang, Q., Gao, H., Yan, D., Peng, H., Xiao, S.: Contributions of moisture sources to precipitation in the major drainage basins in the Tibetan Plateau, Sci. China-Earth Sci. 65, 1088, https://doi.org/10.1007/s11430-021-9890-6, 2022

Link, A., van der Ent, R., Berger, M., Eisner, S., Finkbeiner, M.: The fate of land evaporation - a global dataset, Earth System Science Data 12, 1897-1912, https://doi.org/10.5194/essd-12-1897-2020, 2020

Liu, R., Wang, X., Wang, Z.: Atmospheric moisture sources of drought and wet events during 1979–2019 in the Three-River Source Region, Qinghai-Tibetan Plateau, Theor. Appl. Climatol. 149, 487-499, https://doi.org/10.1007/s00704-022-04058-9, 2022

Liu, R., Wen, J., Wang, X., Wang, Z., Liu, Y.: Case studies of atmospheric moisture sources in the source region of the Yellow River from a Lagrangian perspective, Int. J. Climatol. 42, 1516-1530, https://doi.org/10.1002/joc.7317, 2021

Liu, X., Liu, Y., Wang, X., Wu, G.: Large-Scale Dynamics and Moisture Sources of the Precipitation Over the Western Tibetan Plateau in Boreal Winter, J. Geophys. Res.-Atmos. 125, e2019JD032133, https://doi.org/10.1029/2019JD032133, 2020a

Liu, Y., Lu, M., Yang, H., Duan, A., He, B., Yang, S., Wu, G.: Land–atmosphere–ocean coupling associated with the Tibetan Plateau and its climate impacts, Natl. Sci. Rev. 7, 534-552, https://doi.org/10.1093/nsr/nwaa011, 2020b

Ma, Y., Lu, M., Bracken, C., Chen, H.: Spatially coherent clusters of summer precipitation extremes in the Tibetan Plateau: Where is the moisture from?, Atmos. Res. 237, 104841, https://doi.org/10.1016/j.atmosres.2020.104841, 2020

Pan, C., Zhu, B., Gao, J., Kang, H., Zhu, T.: Quantitative identification of moisture sources over the Tibetan Plateau and the relationship between thermal forcing and moisture transport, Climate Dyn. 52, 181-196, https://doi.org/10.1007/s00382-018-4130-6, 2018

Pisso, I., Sollum, E., Grythe, H., Kristiansen, N.I., Cassiani, M., Eckhardt, S., Arnold, D., Morton, D., Thompson, R.L., Groot Zwaaftink, C.D., Evangeliou, N., Sodemann, H., Haimberger, L., Henne, S., Brunner, D., Burkhart, J.F., Fouilloux, A., Brioude, J., Philipp, A., Seibert, P., Stohl, A.: The Lagrangian particle dispersion model FLEXPART version 10.4, Geosci. Model Dev. 12, 4955-4997, https://doi.org/10.5194/gmd-12-4955-2019, 2019

Qiu, T., Huang, W., Wright, J.S., Lin, Y., Lu, P., He, X., Yang, Z., Dong, W., Lu, H., Wang, B.: Moisture Sources for Wintertime Intense Precipitation Events Over the Three Snowy Subregions of the Tibetan Plateau, J. Geophys. Res.-Atmos. 124, 12708-12725, https://doi.org/10.1029/2019jd031110, 2019

Sodemann, H., Schwierz, C., Wernli, H.: Interannual variability of Greenland winter precipitation sources: Lagrangian moisture diagnostic and North Atlantic Oscillation influence, J. Geophys. Res.-Atmos. 113, D03107, https://doi.org/10.1029/2007JD008503, 2008

Sprenger, M., Wernli, H.: The LAGRANTO Lagrangian analysis tool – version 2.0, Geosci. Model Dev. 8, 2569-2586, https://doi.org/10.5194/gmd-8-2569-2015, 2015

Stein, A.F., Draxler, R.R., Rolph, G.D., Stunder, B.J.B., Cohen, M.D., Ngan, F.: NOAA's HYSPLIT Atmospheric Transport and Dispersion Modeling System, Bull. Amer. Meteorol. Soc. 96, 2059-2078, https://doi.org/10.1175/BAMS-D-14-00110.1, 2016

Sun, B., Wang, H.: Moisture sources of semiarid grassland in China using the Lagrangian particle model FLEXPART, J. Climate 27, 2457-2474, https://doi.org/10.1175/JCLI-D-13-00517.1, 2014

Tuinenburg, O.A., Staal, A.: Tracking the global flows of atmospheric moisture and associated uncertainties, Hydrol. Earth Syst. Sci. 24, 2419-2435, https://doi.org/10.5194/hess-24-2419-2020, 2020

Van der Ent, R.J., Savenije, H.H., Schaefli, B., Steele-Dunne, S.C.: Origin and fate of atmospheric moisture over continents, Water Resour. Res. 46, W09525, https://doi.org/10.1029/2010WR009127, 2010

van der Ent, R.J., Wang-Erlandsson, L., Keys, P.W., Savenije, H.H.G.: Contrasting roles of interception and transpiration in the hydrological cycle – Part 2: Moisture recycling, Earth Syst. Dynam. 5, 471-489, https://doi.org/10.5194/esd-5-471-2014, 2014

Wang, C., Wang, Z.-H., Yang, J., Li, Q.: A Backward-Lagrangian-Stochastic Footprint Model for the Urban Environment, Boundary-Layer Meteorology 168, 59-80, https://doi.org/10.1007/s10546-018-0338-6, 2018

Wang, Y., Yang, K., Huang, W., Qiu, T., Wang, B.: Dominant Contribution of South Asia Monsoon to External Moisture for Extreme Precipitation Events in Northern Tibetan Plateau, Remote Sensing 15, 735, https://doi.org/10.3390/rs15030735, 2023

Winschall, A., Pfahl, S., Sodemann, H., Wernli, H.: Comparison of Eulerian and Lagrangian moisture source diagnostics – the flood event in eastern Europe in May 2010, Atmos. Chem. Phys. 14, 6605-6619, https://doi.org/10.5194/acp-14-6605-2014, 2014

Xu, Y., Gao, Y.: Quantification of Evaporative Sources of Precipitation and Its Changes in the Southeastern Tibetan Plateau and Middle Yangtze River Basin, Atmosphere 10, 428, https://doi.org/10.3390/atmos10080428, 2019

Yang, K., Wu, H., Qin, J., Lin, C., Tang, W., Chen, Y.: Recent climate changes over the Tibetan Plateau and their impacts on energy and water cycle: A review, Glob. Planet. Change 112, 79-91, https://doi.org/10.1016/j.gloplacha.2013.12.001, 2014

Yang, S., Zhang, W., Chen, B., Xu, X., Zhao, R.: Remote moisture sources for 6-hour summer precipitation over the Southeastern Tibetan Plateau and its effects on precipitation intensity, Atmos. Res. 236, 104803, https://doi.org/10.1016/j.atmosres.2019.104803, 2020

https://doi.org/10.5194/egusphere-2024-14
Preprint. Discussion started: 29 January 2024

Yao, S., Jiang, D., Zhang, Z.: Lagrangian simulations of moisture sources for Chinese Xinjiang precipitation during 1979–2018, Int. J. Climatol. 41, E216-E232, https://doi.org/10.1002/joc.6679, 2020

Yao, S., Jiang, D., Zhang, Z.: Moisture Sources of Heavy Precipitation in Xinjiang Characterized by Meteorological Patterns, J. Hydrometeorol. 22, 2213-2225, https://doi.org/10.1175/JHM-D-20-0236.1, 2021

Yao, T., Bolch, T., Chen, D., Gao, J., Immerzeel, W., Piao, S., Su, F., Thompson, L., Wada, Y., Wang, L., Wang, T., Wu, G., Xu, B., Yang, W., Zhang, G., Zhao, P.: The imbalance of the Asian water tower, Nature Reviews Earth & Environment https://doi.org/10.1038/s43017-022-00299-4, 2022

Yao, T., Masson-Delmotte, V., Gao, J., Yu, W., Yang, X., Risi, C., Sturm, C., Werner, M., Zhao, H., He, Y.: A review of climatic controls on δ18O in precipitation over the Tibetan Plateau: Observations and simulations, Rev. Geophys. 51, 525-548, https://doi.org/10.1002/rog.20023, 2013

Yao, T., Xue, Y., Chen, D., Chen, F., Thompson, L., Cui, P., Koike, T., Lau, W.K.-M., Lettenmaier, D., Mosbrugger, V.: Recent Third Pole's rapid warming accompanies cryospheric melt and water cycle intensification and interactions between monsoon and environment: multi-disciplinary approach with observation, modeling and analysis, Bull. Amer. Meteorol. Soc. 100, 423-444, https://doi.org/10.1175/BAMS-D-17-0057.1, 2018

Zhang, C.: Moisture source assessment and the varying characteristics for the Tibetan Plateau precipitation using TRMM, Environ. Res. Lett. 15, 104003, https://doi.org/10.1088/1748-9326/abac78, 2020

Zhang, C., Tang, Q., Chen, D.: Recent changes in the moisture source of precipitation over the Tibetan Plateau, J. Climate 30, 1807-1819, https://doi.org/10.1175/JCLI-D-15-0842.1, 2017

Zhang, C., Tang, Q.H., Chen, D.L., van der Ent, R.J., Liu, X.C., Li, W.H., Haile, G.G.: Moisture Source Changes Contributed to Different Precipitation Changes over the Northern and Southern Tibetan Plateau, J. Hydrometeorol. 20, 217-229, https://doi.org/10.1175/Jhm-D-18-0094.1, 2019a

Zhang, Y., Huang, W., Zhong, D.: Major Moisture Pathways and Their Importance to Rainy Season Precipitation over the Sanjiangyuan Region of the Tibetan Plateau, J. Climate 32, 6837-6857, https://doi.org/10.1175/jcli-d-19-0196.1, 2019b

Zhao, R., Chen, B., Xu, X.: Intensified Moisture Sources of Heavy Precipitation Events Contributed to Interannual Trend in Precipitation Over the Three-Rivers-Headwater Region in China, Frontiers in Earth Science 9, https://doi.org/10.3389/feart.2021.674037, 2021

Zhao, R., Chen, B., Zhang, W., Yang, S., Xu, X.: Moisture source anomalies connected to flood-drought changes over the three-rivers headwater region of Tibetan Plateau, Int. J. Climatol. 43, 5303-5316, https://doi.org/10.1002/joc.8147, 2023

Zhou, Y., Xie, Z., Liu, X.: An Analysis of Moisture Sources of Torrential Rainfall Events over Xinjiang, China, J. Hydrometeorol. 20, 2109-2122, https://doi.org/10.1175/JHM-D-19-0010.1, 2019